# Internal Pressures of Sodium, Potassium, and Rubidium Fluids at Different Temperatures

**Vahid Moeini***

Payame Noor University, Behshahr Center, Behshahr, Iran

In this paper, we calculate internal pressure of sodium, potassium, and rubidium and then use the internal pressure to predict X-ray diffraction and small-angle X-ray scattering to the range where the compressibility of the interacting electron gas has been theoretically predicted to become negative. Isotherms of internal pressure of rubidium fluid versus molar volume show a maximum around 1.152 $g \cdot cm^{-3}$ in agreement with X-ray diffraction and small-angle X-ray scattering. An attempt is made to establish a function for the accurate calculation of the internal pressure and the prediction of metal−nonmetal transition alkali metals based on the internal pressure.

## Introduction

How the physical properties of an alkali metal fluid depend on the structure of that fluid has long been of interest. In the last century, much attention has been paid to the alkali liquid metals such as cesium and rubidium due to their industrial applications. Recent technological advances have yielded increased applications for the alkali metals. An accurate knowledge of the physical properties of these fluids has become vital in many of these applications.[1−5] X-ray diffraction and small-angle X-ray scattering of rubidium fluids have been measured by reducing electron density down to the range where the compressibility of the interacting electron gas has been theoretically predicted to become negative. It suggests that an attractive interaction among like charges, ions in this case, is enhanced.[6] Despite the metallic fluids' applications in industries, they are very complicated at the molecular level.[7−10] Recently, there has been considerable progress in the development of regularities applicable for the metallic fluids. Among these, we refer to a general regularity which has been reported for pure dense fluids, according to which $(Z - 1)V^2$ is linear with respect to $\rho^2$, and each isotherm can be taken as

$$(Z - 1)V^2 = A + B\rho^2 \tag{1}$$

where $Z \equiv pV/RT$ is the compression factor; $\rho = 1/V$ is the molar density; and $A$ and $B$ are the temperature-dependent parameters as follows

$$A = A'' - \frac{A'}{RT} \tag{2}$$

$$B = \frac{B'}{RT} \tag{3}$$

Here $A'$ and $B'$ are related to intermolecular attractive and repulsive forces, respectively, while $A''$ is related to the nonideal thermal pressure and $RT$ has its usual meaning.[11,12] The regularity was originally suggested on the basis of a simple lattice-type model applied to a Lennard-Jones (12, 6) fluid. The linear isotherm regularity, LIR, can be used to predict metal−nonmetal transition.[13]

Another work has derived an equation of state for liquid cesium based on a suggested potential function of Lennard-Jones (6, 3) in accord with the characteristics of large attraction and soft repulsion at the asymptotes of the interaction potentials.[14,15] By considering the interaction of nearest adjacent atoms in a dense fluid, the equation of state predicts that $(Z - 1)V^2$ is linear with respect to $1/\rho$ for each isotherm.

$$(Z - 1)V^2 = C + B(1/\rho) \tag{4}$$

where $C$ and $B$ are temperature-dependent parameters as follows

$$C = C_2 + \frac{C_1}{RT} \tag{5}$$

$$B = -\frac{B_1}{RT} \tag{6}$$

This regularity has been used for a range of metal−nonmetal transitions for liquid cesium.

In the present work, we use the internal pressure to predict experimental regularities in sodium, potassium, and rubidium metals. The internal pressure plays a major role in thermodynamics because it is a measure of the variation of the internal energy of a substance as the volume it occupies is changed at constant temperature.[16] Considering the internal pressure by modeling the average configurational potential energy and then taking its derivative with respect to volume predicts that the isotherm $((\partial E/\partial V)_T/\rho RT)V^2$ is a linear function of $\rho^2$, where $E$ is the internal energy and $(\partial E/\partial V)_T$ is the internal pressure.[17] The final result is therefore of the form

* Author to whom correspondence should be addressed. E-mail: v_moeini@yahoo.com.

10.1021/je100627c 
Published on Web 11/19/2010

$$\left(\frac{(\partial E/\partial V)_T}{\rho RT}\right)V^2 = A + B\rho^2 \tag{7}$$

where the intercept $A$ and the slope $B$ are related to attraction and repulsion, respectively, and both depend on temperature. In practice, it shows that

$$A = \frac{A_1}{RT} \tag{8}$$

$$B = B_2 - \frac{B_1}{RT} \tag{9}$$

Thus, the intercept $A$ and the slope $B$ are linear in $1/T$. The purpose of this paper is to point out that this general regularity applies to alkali metals. The regularity can be used for predicting a metal−nonmetal transition in alkali metals. When the transition occurs, $((\partial E/\partial V)_T/\rho RT)V^2$ is nonlinear in $\rho^2$ for alkali metals that are similar to LIR behavior.

The other fact which has been investigated in this work is a new regularity that has been used for a range of metal−nonmetal transitions of alkali metals based on the internal pressures that are calculated by the Lennard-Jones (6-3) potential function.[18] In this paper, we report new accurate measurements of the internal pressure of sodium, potassium, and rubidium made at wide pressures and temperatures, and we also use the internal pressure to predict experimental regularities in sodium, potassium, and rubidium metals.

Finally, we have performed a structural study of the expanded fluid rubidium based on internal pressure. The experimental results show that the internal pressure maximum occurs at around 1.152 g·cm$^{-3}$ or 74 cm$^3$·mol$^{-1}$ in accord with X-ray diffraction and small-angle X-ray scattering measurements.[6] These structural features suggest that clustering occurs in the metallic fluid. We also show that the internal pressure expansion of alkali metal diagrams is similar to the Maxwell−Boltzmann distribution or temperature−composition diagrams for systems that consist of pairs of partially miscible liquids.

## Theory

In the present work, we approximate the average potential energy by summing the contribution from the nearest neighbors only, assuming single inverse powers for the effective repulsion and attraction, i.e.

$$U = \frac{N}{2}z(\rho)\left(\frac{C_n}{\bar{r}^n} - \frac{C_m}{\bar{r}^m}\right) \tag{10}$$

where $U$ is the total potential energy among $N$ molecules; $z(\rho)$ is the average number of nearest neighbors; $\bar{r}$ is average distance between nearest neighbors; and $C_n$ and $C_m$ are constants.[11] For a repulsive−attractive $(n,m)$ potential, adjustable parameters $n$ and $m$ represent exponents of repulsion and attraction interactions, respectively. It is well-known that $z(\rho)$ is proportional to $\rho$, as is the case for liquid argon, rubidium, and cesium, and taking $v \approx \bar{r}^3$, $U$ can be written as

$$\frac{U}{N} = \frac{K_n}{v^{n/3+1}} - \frac{K_m}{v^{m/3+1}} \tag{11}$$

where $K_n$ and $K_m$ are constants. Carrying out the differentiation, we obtain the internal pressure for dense fluids.

$$p_{\text{int}} = \left(\frac{\partial E}{\partial V}\right)_T \approx \left[\frac{\partial (U/N)}{\partial v}\right]_T = A_1\rho^{m/3+2} - B_1\rho^{n/3+2} \tag{12}$$

where $A_1$ and $B_1$ are constants. To determine the potential type, the coefficient of determination ($R^2$) evaluates for liquid sodium, potassium, and rubidium.[17,18] The results show that not only cesium but also all alkali metals obey the Lennard-Jones (6-3) potential function in the whole liquid range including the metal−nonmetal transition.[14,18] It is a fact that any kinetic energy contribution to the internal energy $E$ will vanish on taking the derivative since the temperature is held constant. We use with the exact thermodynamic relation[19]

$$(\partial E/\partial V)_T = T(\partial p/\partial T)_\rho - p \tag{13}$$

in which $T(\partial p/\partial T)_\rho$ is usually called the thermal pressure. It has proved eqs 7 to 9, and the final result is therefore of the form

$$\left(\frac{(\partial E/\partial V)_T}{\rho RT}\right)V^2 = A + B\left(\frac{1}{\rho}\right) \tag{14}$$

where the intercept $A$ and the slope $B$ are related to repulsion and attraction, respectively, and both depend on temperature. In practice, it has been shown that the intercept $A$ and the slope $B$ are functions in $1/T$.[18]

## Experimental Test

Initially, we present here a simple method of the ideas and use the thermal pressure coefficient directly in place of using an equation of state to analyze experimental $pVT$ data. The equation of state described in this paper is explicit in Helmholtz energy $\nabla$ with the two independent variables density $\rho$ and $T$. At a given temperature, the pressure can be determined by the Helmholtz energy.[17,18]

$$p(T,\rho) = -\left(\frac{\partial \nabla}{\partial V}\right)_T \tag{15}$$

Using the general expression of the relation to the reduced Helmholtz energy $\phi = \nabla/(RT)$ and its derivatives then gives

$$p^{\text{r}}(\delta,\tau) = 1 + \delta\phi_\delta{}^{\text{r}} \tag{16}$$

where $p^{\text{r}}(\delta,\tau) = p(\delta,\tau)/\rho RT$ is the reduced pressure; $\delta = \rho/\rho_{\text{C}}$ is the reduced density; and $\tau = T_{\text{C}}/T$ is the inverse reduced temperature. Both the density $\rho$ and the temperature $T$ are reduced with their critical values $\rho_{\text{C}}$ and $T_{\text{C}}$, respectively. Since the Helmholtz energy as a function of density and temperature is one of the four fundamental forms of an equation of state, all the thermodynamic properties of a pure substance can be obtained by combining derivatives of the reduced Helmholtz energy $\phi$. Here $\phi_\delta$ and $\phi_\delta{}^{\text{r}}$ are defined as.

$$\phi_\delta = \left(\frac{\partial \phi}{\partial \delta}\right)_\tau \tag{17}$$

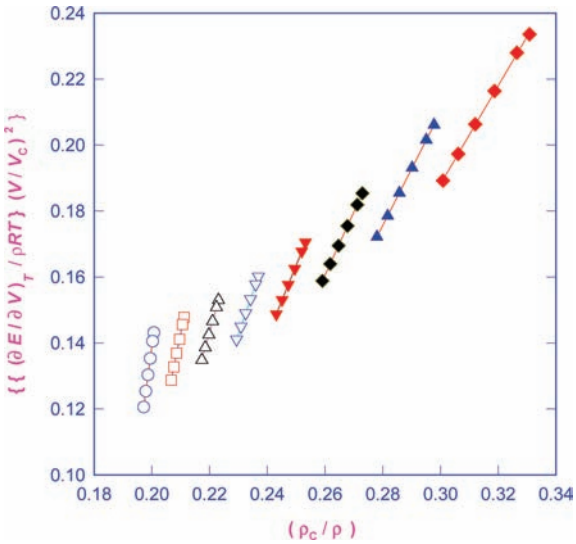


**Figure 1.** Validity of the linearity of $((\partial E/\partial V)_T/\rho RT)V^2$ vs $(1/\rho)$ for different isotherms of Na in the range of (500 to 2000) K: ○, 500 K; □, 700 K; Δ, 900 K; ▽, 1100 K; red ▼, 1300 K; black ♦, 1500 K; blue ▲, 1700 K; red ♦, 1900 K.

and

$$\phi_\delta^{\,r} = \left(\frac{\partial \phi^r}{\partial \delta}\right)_\tau \tag{18}$$

and

$$d\tau = -\frac{T_c}{T^2}dT \tag{19}$$

The above procedure leads to the acquisition of the thermal pressure coefficient from the reduced Helmholtz energy for real fluids.

$$\left(\frac{\partial p}{\partial T}\right)_\delta = \rho R\left[(1 + \delta\phi_\delta^{\,r}) - \delta\tau\left(\frac{\partial \phi_\delta^{\,r}}{\partial \tau}\right)_\delta\right] \tag{20}$$

First, for an experimental test, a regularity that has been used for a range of metal−nonmetal transitions of the alkali metals is derived by the Lennard-Jones (6-3) potential function and using experimental data. In Figure 1, the isotherms are plotted for liquid Na in the range (500 to 2000) K. The intercept $A$ and the slope $B$ are related to repulsion and attraction, respectively, and both depend on temperature.[18] Thus, the intercept $A$ and the slope $B$ are functions in $1/T$. This result immediately shows why $A$ and $B$ have such similarity to the second virial coefficient, which has the same temperature dependence as that of a van der Waals gas, whose second virial coefficient is $b - a/RT$.[11] In this paper, we applied Na liquid for our primary test of the linear parameters of the isotherms in eq 14 using the experimental $pVT$ data. The linear parameters of the isotherms of internal pressure and relative uncertainty in accordance with eq 14 for liquid Na are also shown in Table 1. To test the usefulness of these results, we have showed relative uncertainty of Na in Figure 2 that does not exceed 0.22 %.

This test has also been repeated for liquid potassium in the range (500 to 1800) K in Figures 3 and 4 and for liquid rubidium in the range of (500 to 1500) K in Figures 5 and 6. In this

**Table 1. Equation of $((\partial E/\partial V)_T/\rho RT)(v/v_C)^2 = A + B(\rho_C/\rho)$, Reduced Intercept ($A$) and Slope ($B$), the Maximum Relative Error Defined by $[((\partial E/\partial v)_{T,\text{exptl}} - (\partial E/\partial v)_{T,\text{calcd}})/\{(\partial E/\partial v)_{T,\text{exptl}}\}]\cdot 100$, and the Pressure Range ($\Delta p$) of the Data for Na[a]**

| $T$ | | | max relative error | $\Delta p$ |
|---|---|---|---|---|
| K | $A$ | $B$ | (%) | MPa |
| 500 | −1.1410 | 6.3991 | 0.04 | 10 to 100 |
| 600 | −0.9160 | 5.1592 | 0.05 | 10 to 100 |
| 700 | −0.7516 | 4.2596 | 0.06 | 10 to 100 |
| 800 | −0.6341 | 3.6159 | 0.06 | 10 to 100 |
| 900 | −0.5497 | 3.1500 | 0.02 | 10 to 100 |
| 1000 | −0.4849 | 2.7909 | 0.02 | 10 to 100 |
| 1100 | −0.4372 | 2.5216 | 0.03 | 10 to 100 |
| 1200 | −0.4011 | 2.3128 | 0.02 | 10 to 100 |
| 1300 | −0.3748 | 2.1533 | 0.02 | 10 to 100 |
| 1400 | −0.3538 | 2.0227 | 0.05 | 10 to 100 |
| 1500 | −0.3368 | 1.9129 | 0.03 | 10 to 100 |
| 1600 | −0.3218 | 1.8158 | 0.04 | 10 to 100 |
| 1700 | −0.3059 | 1.7196 | 0.01 | 10 to 100 |
| 1800 | −0.2876 | 1.6194 | 0.04 | 10 to 100 |
| 1900 | −0.2584 | 1.4885 | 0.22 | 10 to 100 |
| 2000 | −0.2370 | 1.3885 | 0.12 | 10 to 100 |

[a] Data from refs 20 and 21.

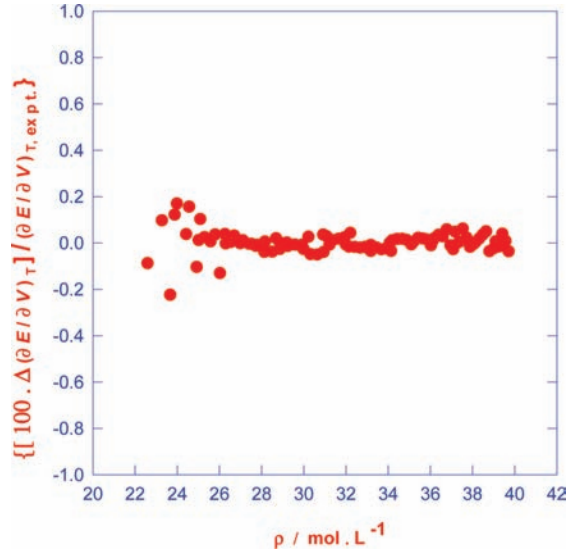


**Figure 2.** Fractional deviations $\Delta(\partial E/\partial v)_T = (\partial E/\partial v)_{T,\text{exptl}} - (\partial E/\partial v)_{T,\text{calcd}}$ of the experimental internal pressure $(\partial E/\partial v)_{T,\text{exptl}}$ of sodium at (500 to 2000) K from values $(\partial E/\partial v)_{T,\text{calcd}}$ obtained with eq 14.

entire range, the deviations from the experimental data do not exceed the estimated relative uncertainty of 0.20 % and 0.35 % for potassium and rubidium, respectively. The linear parameters of the isotherms of internal pressure using eq 14 for liquids potassium and rubidium have been shown in Tables 2 and 3, respectively.

For comparison, the coefficient of determination and the isotherms of internal pressure of the Lennard-Jones (6-3) potential function are compared with the same isotherms of internal pressures that are calculated using the Lennard-Jones (9-6) and (12-6) potential functions. This comparison has been shown in Figures 7, 8, and 9 for liquid sodium, potassium, and rubidium, respectively. Isotherms of internal pressure of the Lennard-Jones (6-3) potential function are perfectly linear in the metal−nonmetal transition range. It also shows that at low temperatures the application of the isotherms of internal pressure that are derived from the (6-3) potentials are equal with the same isotherms of internal pressures that are derived using the Lennard-Jones (9-6) and (12-6) potential functions, while at high temperatures for the Lennard-Jones (9-6) and (12-6) potential

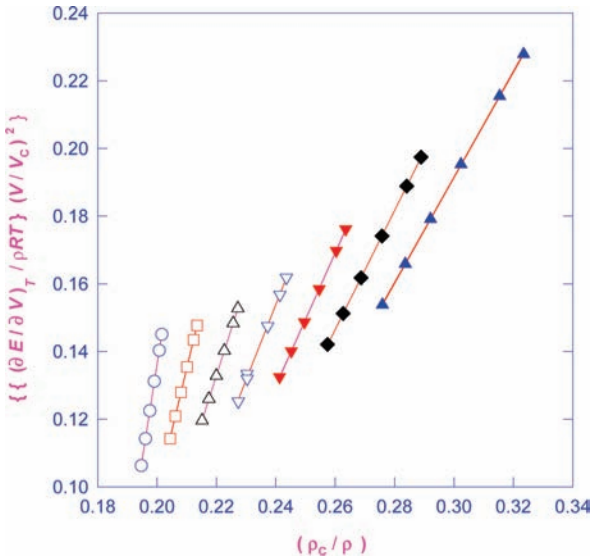


**Figure 3.** Validity of the linearity of the $((\partial E/\partial V)_T/\rho RT)V^2$ vs $(1/\rho)$ for different isotherms of K in the range of (500 to 1800) K: ○, 500 K; □, 700 K; Δ, 900 K; ▽, 1100 K; red ▼, 1300 K; black ♦, 1500 K; blue ▲, 1700 K.

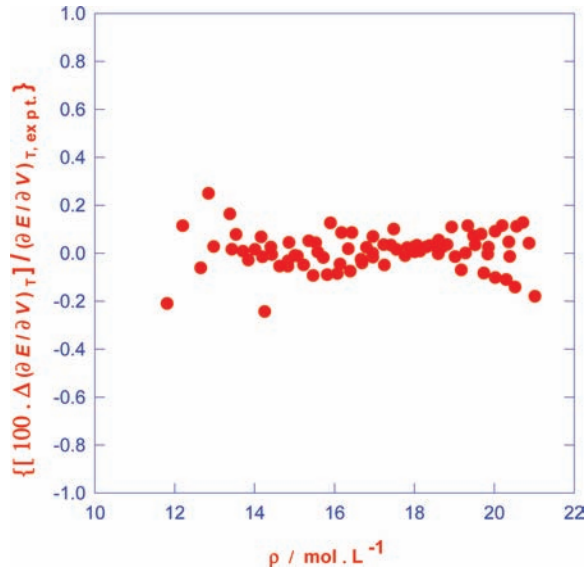


**Figure 4.** Fractional deviations $\Delta(\partial E/\partial v)_T = (\partial E/\partial v)_{T,\text{exptl}} - (\partial E/\partial v)_{T,\text{calcd}}$ of the experimental internal pressure $(\partial E/\partial v)_{T,\text{exptl}}$ of potassium at (500 to 1800) K from values $(\partial E/\partial v)_{T,\text{calcd}}$ obtained with eq 14.

functions, significant deviations in the coefficient of determination are observed. Much of this effort concerns the metal−nonmetal transition, which occurs in the liquid when it is made to expand by heating. Therefore, any potential function harder than the Lennard-Jones (6-3) potential function will deviate from the linear behavior more than the (6-3) isotherm of internal pressure over the whole liquid range. Comparison of the coefficient of determination reveals that the interaction potential in liquid sodium, potassium, and rubidium, both at low temperature and at high temperature, is modeled accurately by the Lennard-Jones (6-3) potential function. This makes the isotherms of internal pressure persist as being linear in both the metallic and nonmetallic regions.

## Prediction of Metal−Nonmetal Transition Alkali Metals by Internal Pressure

Now we show the diagram of internal pressure in an expanding sodium, potassium, and rubidium fluid in accord with

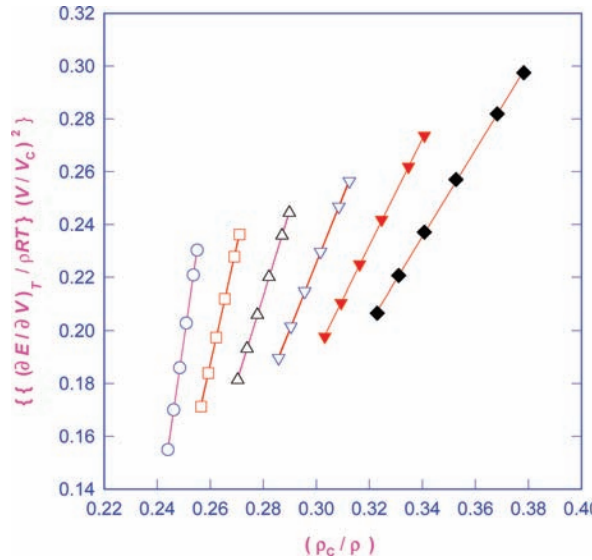


**Figure 5.** Validity of the linearity of the $((\partial E/\partial V)_T/\rho RT)V^2$ vs $(1/\rho)$ for different isotherms of Rb in the range of (500 to 1600) K: ○, 500 K; □, 700 K; Δ, 900 K; ▽, 1100 K; red ▼, 1300 K; black ♦, 1500 K.

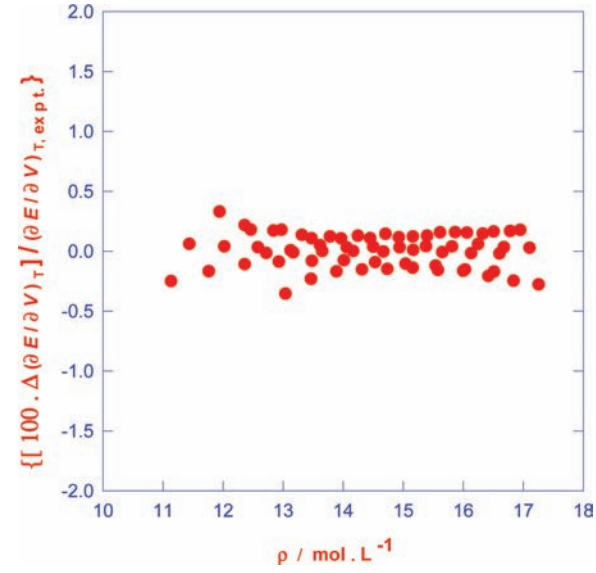


**Figure 6.** Fractional deviations $\Delta(\partial E/\partial v)_T = (\partial E/\partial v)_{T,\text{exptl}} - (\partial E/\partial v)_{T,\text{calcd}}$ of the experimental internal pressure $(\partial E/\partial v)_{T,\text{exptl}}$ of rubidium at (500 to 1600) K from values $(\partial E/\partial v)_{T,\text{calcd}}$ obtained with eq 14.

the Maxwell−Boltzmann distribution diagrams or the temperature−composition diagrams for systems that consist of pairs of partially miscible liquids, which are liquids that do not mix in all proportions at all temperatures. The upper critical solution temperature is the highest temperature at which phase separation occurs. Above the upper critical temperature, the two components are fully miscible. The region below the curve corresponds to the compositions and temperatures at which the liquids form two phases. One example is the nitrobenzene + hexane system.[22] The upper critical solution temperature in the temperature−composition diagrams corresponds to the metal−nonmetal transition temperature in the internal pressure−molar volume diagram. Therefore, in this paper, we propose a new mechanism for prediction of the metal−nonmetal transition which includes a maximum point at isotherms of internal pressure of the alkali fluid versus molar volume at the transition point. This effective procedure considers that the nuclei are completely shielded by core electrons and partially by delocalized valence electrons for alkali metals. However, the cohesion mechanism of these metals

**Table 2. Equation of $((\partial E/\partial V)_T/\rho RT)(v/v_C)^2 = A + B(\rho_C/\rho)$, Reduced Intercept ($A$) and Slope ($B$), the Maximum Relative Error Defined by $[((\partial E/\partial v)_{T,exptl} - (\partial E/\partial v)_{T,calcd})/\{(\partial E/\partial v)_{T,exptl}\}]\cdot 100$, and the Pressure Range ($\Delta p$) of the Data for K[a]**

| $T$ | | | max relative error | $\Delta p$ |
|---|---|---|---|---|
| K | $A$ | $B$ | (%) | MPa |
| 500 | −0.9872 | 5.6170 | 0.18 | 10 to 100 |
| 600 | −0.7780 | 4.4582 | 0.14 | 10 to 100 |
| 700 | −0.6378 | 3.6802 | 0.10 | 10 to 100 |
| 900 | −0.4711 | 2.7455 | 0.05 | 10 to 100 |
| 1000 | −0.4223 | 2.4634 | 0.03 | 10 to 100 |
| 1100 | −0.3870 | 2.2531 | 0.05 | 10 to 100 |
| 1200 | −0.3615 | 2.0933 | 0.10 | 10 to 100 |
| 1300 | −0.3411 | 1.9626 | 0.08 | 10 to 100 |
| 1400 | −0.3251 | 1.8551 | 0.09 | 10 to 100 |
| 1500 | −0.3102 | 1.7566 | 0.13 | 10 to 100 |
| 1600 | −0.2948 | 1.6612 | 0.05 | 10 to 100 |
| 1700 | −0.2762 | 1.5589 | 0.09 | 10 to 100 |
| 1800 | −0.2522 | 1.4435 | 0.20 | 10 to 100 |

[a] Data from refs 20 and 21.

**Table 3. Equation of $((\partial E/\partial V)_T/\rho RT)(v/v_C)^2 = A + B(\rho_C/\rho)$, Reduced Intercept ($A$) and Slope ($B$), the Maximum Relative Error Defined by $[((\partial E/\partial v)_{T,exptl} - (\partial E/\partial v)_{T,calcd})/\{(\partial E/\partial v)_{T,exptl}\}]\cdot 100$, and the Pressure Range ($\Delta p$) of the data for Rb[a]**

| $T$ | | | max relative error | $\Delta p$ |
|---|---|---|---|---|
| K | $A$ | $B$ | (%) | MPa |
| 500 | −1.5189 | 6.8593 | 0.28 | 10 to 100 |
| 600 | −1.1984 | 5.4496 | 0.25 | 10 to 100 |
| 700 | −0.9750 | 4.4700 | 0.21 | 10 to 100 |
| 800 | −0.8130 | 3.7611 | 0.16 | 10 to 100 |
| 900 | −0.6922 | 3.2326 | 0.16 | 10 to 100 |
| 1000 | −0.5990 | 2.8248 | 0.15 | 10 to 100 |
| 1100 | −0.5255 | 2.5031 | 0.15 | 10 to 100 |
| 1200 | −0.4656 | 2.2415 | 0.15 | 10 to 100 |
| 1300 | −0.4142 | 2.0193 | 0.18 | 10 to 100 |
| 1400 | −0.3679 | 1.8239 | 0.23 | 10 to 100 |
| 1500 | −0.3233 | 1.6430 | 0.35 | 10 to 100 |

[a] Data from refs 20 and 21.

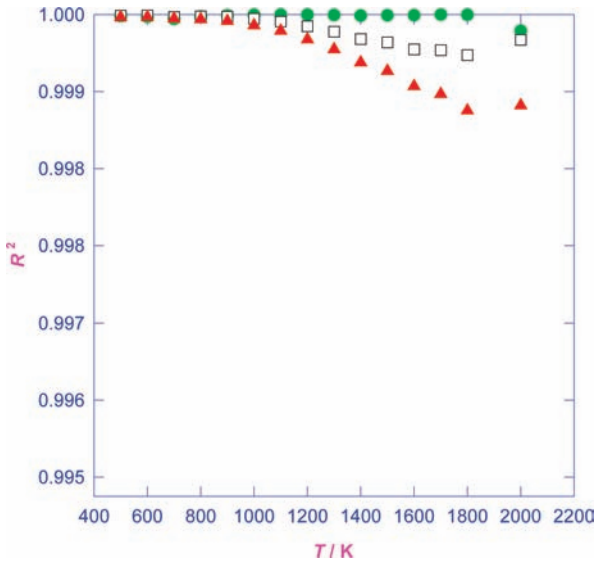


**Figure 7.** Coefficient of determination ($R^2$) and the same isotherms of internal pressure, calculated using the (6-3), (9-6), and (12-6) Lennard-Jones potential functions of Na in the range of (500 to 2000) K: green ●, (6-3); □, (9-6); red ▲, (12-6) Lennard-Jones potential functions.

will be suppressed by a localization of electrons, and the metallic character is gradually changed to a nonmetallic kind. In the liquid phase, on the other hand, the metal liquid is mixed in all proportions of mainly neutral atoms plus ions and molecules comprising clusters of different size.

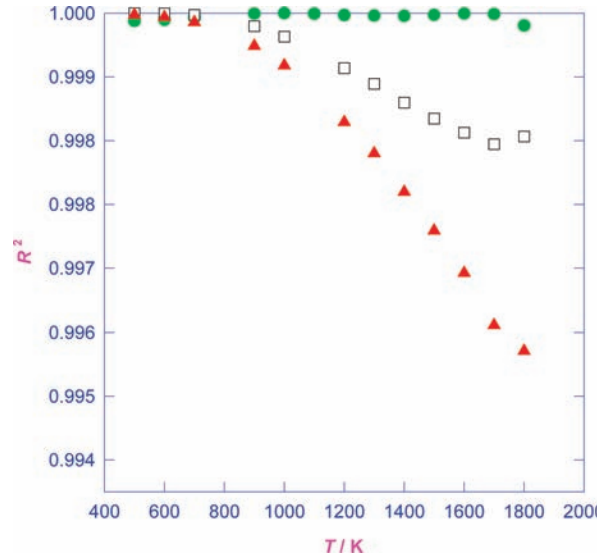


**Figure 8.** Coefficient of determination ($R^2$) and the same isotherms of internal pressure, calculated using the (6-3), (9-6), and (12-6) Lennard-Jones potential functions of K in the range of (500 to 1800) K: green ●, (6-3); □, (9-6); red ▲, (12-6) Lennard-Jones potential functions.

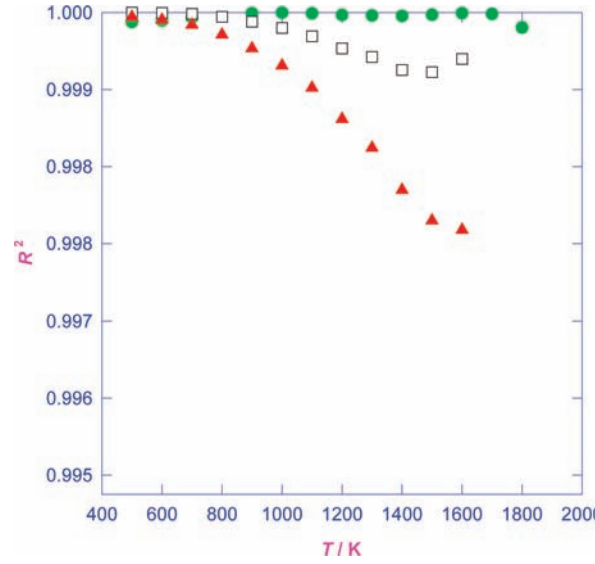


**Figure 9.** Coefficient of determination ($R^2$) and the same isotherms of internal pressure, calculated using the (6-3), (9-6), and (12-6) Lennard-Jones potential functions of Rb in the range of (500 to 1600) K: green ●, (6-3); □, (9-6); red ▲, (12-6) Lennard-Jones potential functions.

We have calculated and plotted the internal pressure versus molar volume at various temperatures for sodium (Figure 10). Isotherms of internal pressure of the sodium fluid versus molar volume show a maximum point at around 0.6802 $g\cdot cm^{-3}$ or 33.8 $cm^3\cdot mol^{-1}$ that corresponds to 1500 K. It shows that below 1500 K the application of the isotherms of internal pressure is equal with the same repulsion, while beyond 1500 K, a significant slope sign that corresponds to attraction for the internal pressure is observed. Much of this effort concerns the metal−nonmetal transition which occurs in the liquid when it is made to expand by heating.

We have also calculated and plotted the internal pressure of the potassium fluid versus molar volume at various temperatures (Figure 11). Isotherms of internal pressure of the potassium fluid versus molar volume show a maximum point at around 0.6043 $g\cdot cm^{-3}$ or 64.7 $cm^3\cdot mol^{-1}$ which corresponds to 1400 K. We have also calculated and plotted the internal pressure of the

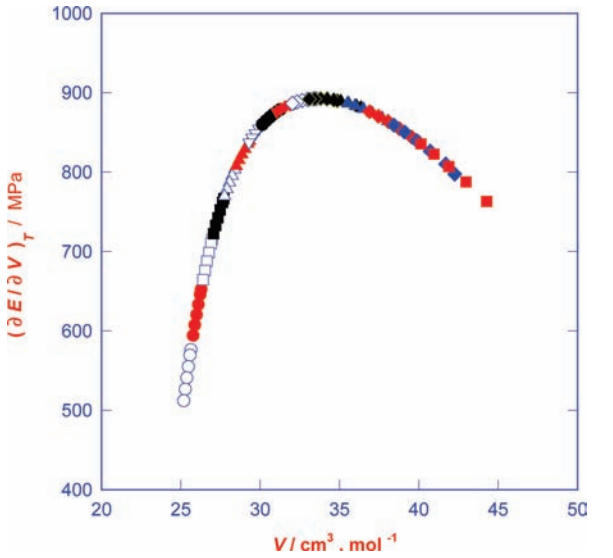


**Figure 10.** Internal pressures for expanded fluid sodium at various temperatures and pressures: ○, 500 K; red ●, 600 K; □, 700 K; black ■, 800 K; Δ, 900 K; red ▲, 1000 K; ▽, 1100 K; black ●, 1200 K; red ▼, 1300 K; ◊, 1400 K; black ♦, 1500 K; black ▲, 1600 K; blue ▲, 1700 K; red ♦, 1800 K; blue ♦, 1900 K; red ■, 2000 K.

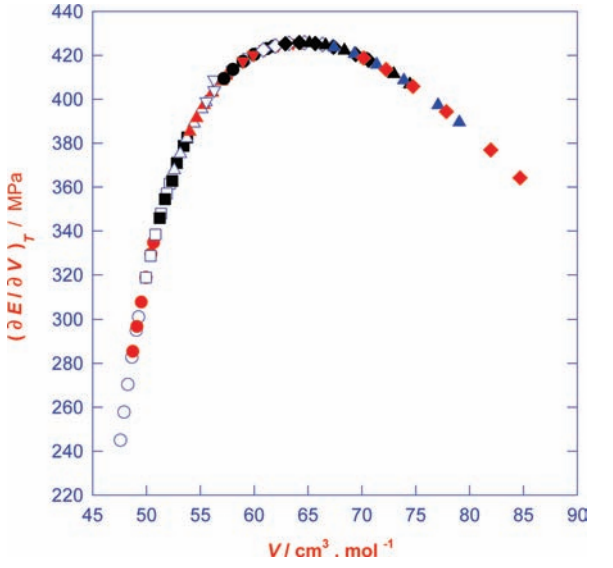


**Figure 11.** Internal pressures for expanded fluid potassium at various temperatures and pressures: ○, 500 K; red ●, 600 K; □, 700 K; black ■, 800 K; Δ, 900 K; red ▲, 1000 K; ▽, 1100 K; black ●, 1200 K; red ▼, 1300 K; ◊, 1400 K; black ♦, 1500 K; black ▲, 1600 K; blue ▲, 1700 K; red ♦, 1800 K.

rubidium fluid versus molar volume at various temperatures (Figure 12). Isotherms of internal pressure of the rubidium fluid versus molar volume show a maximum point at around 1.152 g·cm$^{-3}$ or 74 cm$^3$·mol$^{-1}$ corresponding to 1200 K which corresponds to spatial atomic-density fluctuations and an unusual behavior for the nearest-neighbor distance and coordination number for the rubidium fluid of around 1.1 g·cm$^{-3}$. These structural features suggest that clustering occurs in the metallic fluid accompanying spatial atomic-density fluctuations.[6,23,24] While the transition is occurring, a number of changes similar to the coordination number in the liquid structure happen, and therefore a deviation from the linearity predicted by the coefficient of determination and of the isotherms of internal pressure of the Lennard-Jones (12-6) potential function for a single-phase system is observed.[13]

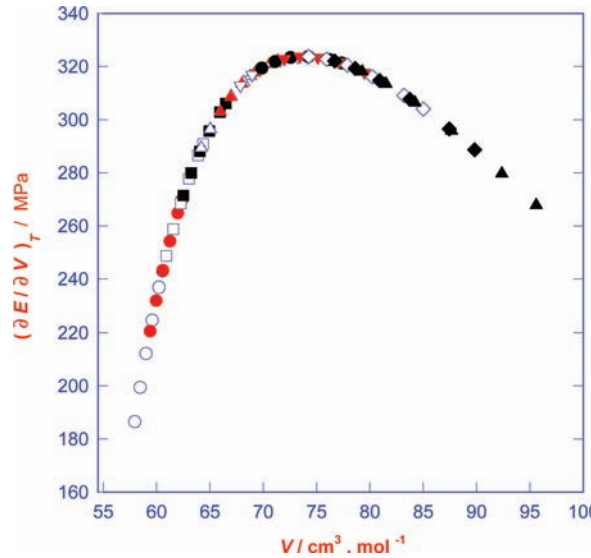


**Figure 12.** Internal pressures for expanded fluid rubidium at various temperatures and pressures: ○, 500 K; red ●, 600 K; □, 700 K; black ■, 800 K; Δ, 900 K; red ▲, 1000 K; ▽, 1100 K; black ●, 1200 K; red ▼, 1300 K; ◊, 1400 K; black ♦, 1500 K; black ▲, 1600 K.

A comparison of Figures 10 to 12 shows that the range of volumes broadens as the metal atomic mass increases. Heavier alkali atoms also have a broader distribution of volumes than light atoms.

## Results and Discussion

The Maxwell−Boltzmann distribution is one of the most important relationships in all of physical science. Historically, it predated the more general Boltzmann distribution of energy-level populations, one of the cornerstones of applied statistical mechanics, of which is of course a special case. We shall find similarity between the Maxwell−Boltzmann distribution diagram and the internal pressure−molar volume diagram of metals.

The linear isotherm regularity, LIR, has been used to predict metal−nonmetal transition. During the transition, a number of changes in the liquid structure occur, and therefore a deviation from the linearity predicted by the LIR for a single-phase system is observed. The statistical mechanical theory of the mixture, along with the LIR, has been used to derive an appropriate equation of state for a mixture of metal and nonmetal, after the beginning of the transition. However, it is the idea that the cause of deviation of LIR isotherms in expanded liquid alkali metals in the transition region is due to the underestimation of extra attractive potential due to development of polarized metal atoms in addition to polyatomic clusters.[11,13]

In another work, it has been shown that a regularity $((\partial E/\partial V)_T/\rho RT)V^2$ is a linear function of $\rho^2$ for each isotherm as both compressed liquids and dense supercritical fluids are based on the Lennard-Jones (12-6) potential function.[17] In the present paper, using internal pressure regularity based on the Lennard-Jones (12-6) potential function to sodium, potassium, and rubidium metal liquids shows that isotherms deviate from linear behavior as the transition temperature (about 1500 K for sodium, 1400 K for potassium, and 1200 K for rubidium) is approached.[17] Therefore, we have shown in this work that using internal pressure based on the Lennard-Jones (12-6) potential similar to the equation of state based on the Lennard-Jones (12-6) potential function predicts a metal−nonmetal transition in

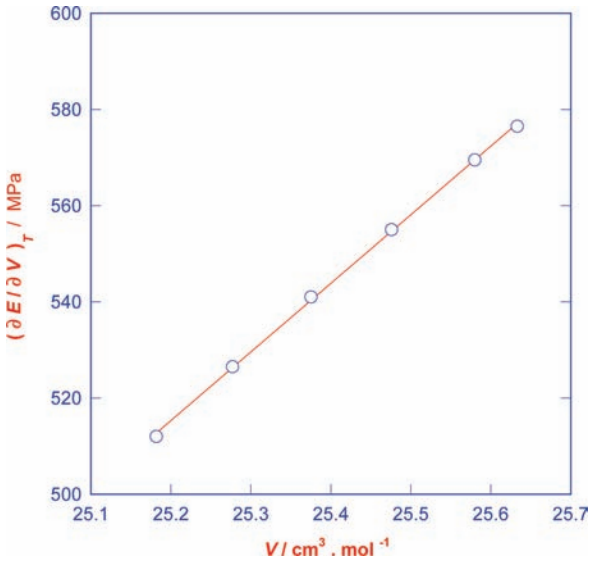


**Figure 13.** Internal pressures for expanded fluid sodium before transition temperature: ○, 500 K.

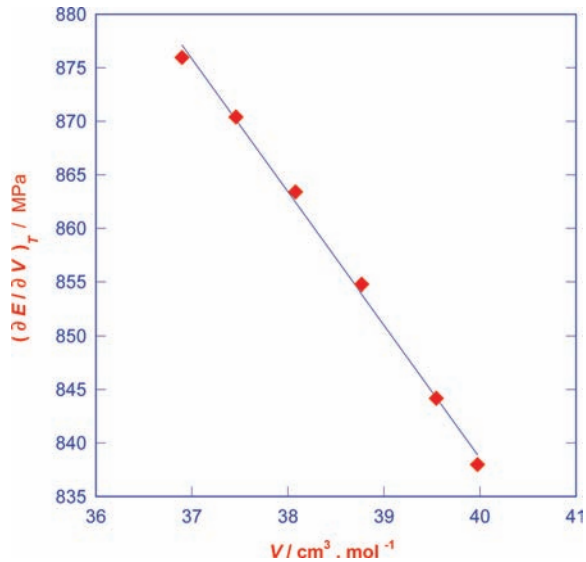


**Figure 14.** Internal pressures for expanded fluid sodium after transition temperature: red ♦, 1800 K.

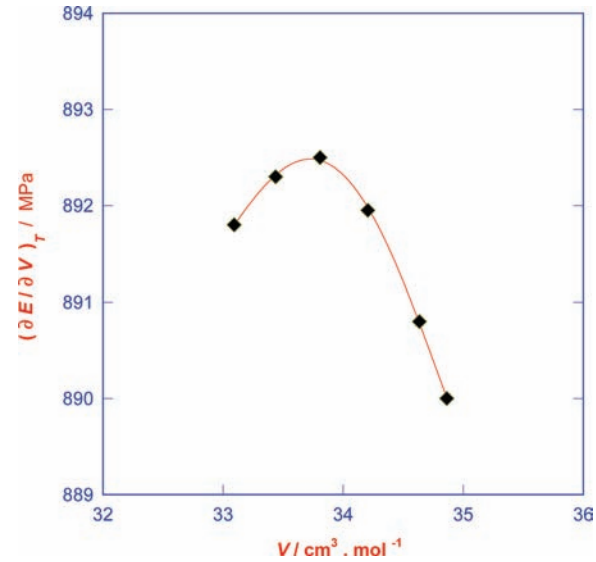


**Figure 15.** Internal pressures for expanded fluid sodium at transition temperature: ♦, 1500 K.

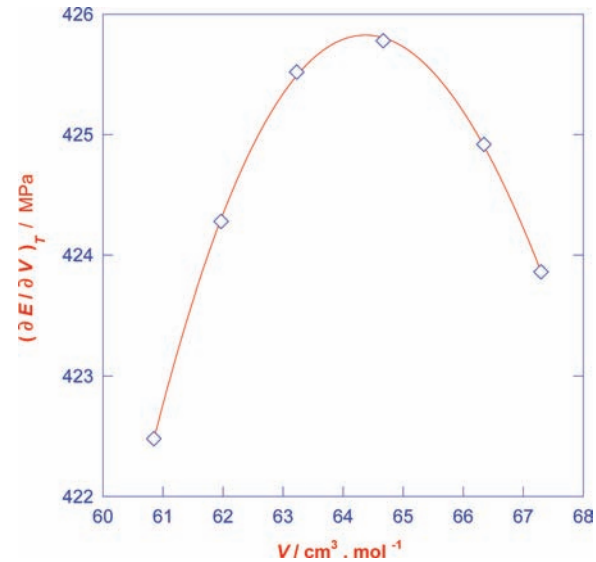


**Figure 16.** Internal pressures for expanded fluid potassium at transition temperature: ◇, 1400 K.

alkali metals.[13] The predictions are in agreement with experimental observations.

In this paper, we have also shown that the Lennard-Jones (6-3) potential function could account for calculation of the internal pressures, particularly in the range that a liquid metal turns into the corresponding nonmetal.[14] Therefore, we have predicted in this work that using internal pressure based on the Lennard-Jones (6-3) potential similar to an equation of state based on the Lennard-Jones (6-3) potential function remains linear over the entire liquid range including the metal−nonmetal transition range. The predictions are in agreement with experimental observations.[18]

Finally, we have performed a structural study of the expanded sodium, potassium, and rubidium fluid based on internal pressure. Isotherms of internal pressure are fairly linear for expanded fluid alkali metals before and after transition temperatures (Figures 13 and 14, respectively), and they only show a maximum point at transition temperature. The experimental results show that the maximum point of the internal pressure is at around 0.6802 g·cm$^{-3}$ or 33.8 cm$^3$·mol$^{-1}$, 0.6043 g·cm$^{-3}$ or 64.7 cm$^3$·mol$^{-1}$, and 1.152 g·cm$^{-3}$ or 74 cm$^3$·mol$^{-1}$, for sodium, potassium, and rubidium in Figures 15, 16, and 17, respectively. Therefore, the structural features of the expanded fluid alkali metals such as local contraction and appearance of the internal pressure maximum in the metallic state at around maximum might be caused by the enhancement in the attractive interaction among the ions and interpreted as the emergence of such an inhomogeneous state induced by the negative sign of the dielectric function of the gas, and it can also be caused spatial atomic-density fluctuations and an unusual behavior for the nearest-neighbor distance and coordination number for the Rb fluid of around 1.1 g·cm$^{-3}$.[6,23,24]

## Conclusion

In the present work, the internal pressures of sodium, potassium, and rubidium for a wide range of temperatures are derived from density using the Helmholtz energy, which is based on using the (6-3) Lennard-Jones potential function.[17,18] The density dependence of internal pressure derived for liquid sodium, potassium, and rubidium shows features in common

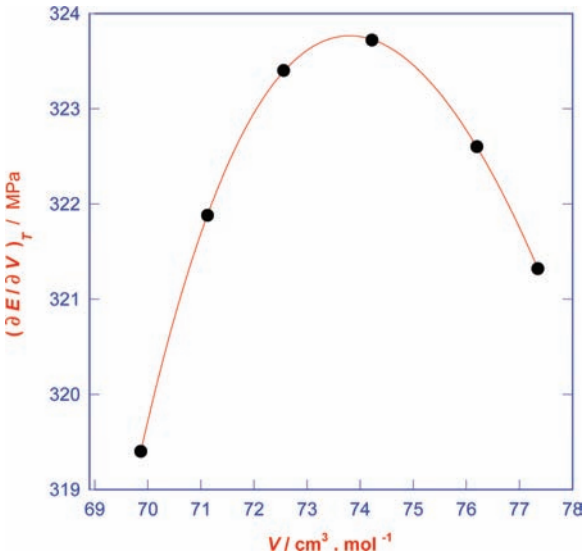


**Figure 17.** Internal pressures for expanded fluid rubidium at transition temperature: ●, 1200 K.

with that for liquid cesium, such that with decreasing density the repulsive part of the internal pressure becomes softer and the resulting attractive part grows longer.[14,18]

The other fact which has been investigated in this work is a new method for prediction of metal−nonmetal transition not only for cesium fluid but also for all alkali metals based on Lennard-Jones potential functions and using the internal pressure results. The internal pressure of an element is the main criteria for its metallic or nonmetallic character[13,18]

We shall also find many applications of the Maxwell−Boltzmann distribution to the internal pressure of metals. The spread of the distribution, which can be described by, say, its width at half the maximum height, is a function of the softened repulsion branch of potential or the metal molecular mass. For a given metal alkali, as the softened repulsion branch of potential or the metal molecular mass increases, the spread of the distribution increases.

## Literature Cited

(1) Ewing, C. T.; Spann, J. R.; Stone, J. P.; Miller, R. R. Pressure-Volume-Temperature relationships for cesium vapor. *J. Chem. Eng. Data* **1971**, *16*, 27–30.
(2) Ewing, C. T.; Spann, J. R.; Stone, J. P.; Steinkuller, E. W.; Miller, R. R. Saturation pressures of cesium to temperatures of pressures approaching critical state. *J. Chem. Eng. Data* **1971**, *16*, 508–510.
(3) Weatherford, W. D.; Johnston, R. K.; Valtierra, M. L. Kinematic viscosity of liquid rubidium from 670° to 688 °C. *J. Chem. Eng. Data* **1964**, *9*, 520–524.
(4) Roehlich, F.; Tepper, F., Jr.; Rakin, R. L. Surface tension of four alkali metals to 1000 °C. *J. Chem. Eng. Data* **1968**, *13*, 518–521.
(5) Monnin, C.; Dubois, M. Thermodynamics of the LiOH + $H_2O$ system. *J. Chem. Eng. Data* **2005**, *50*, 1109–1113.
(6) Mutsuda, K.; Tamura, K.; Inui, M. Instability of the electron gas in an expanding metal. *Phys. Rev. Lett.* **2007**, *98*, 096401−4.
(7) Roehlich, F.; Tepper, F., Jr.; Rakin, R. L. Surface tension of four alkali metals to 1000 °C. *J. Chem. Eng. Data* **1968**, *13*, 518–521.
(8) Stone, J. P.; Ewing, C. T.; Karp, R. L.; Spann, J. R.; Miller, R. R. Predicted high-temperature properties of rubidium. *J. Chem. Eng. Data* **1967**, *12*, 352–356.
(9) Stone, J. P.; Ewing, C. T.; Spann, J. R.; Steinkuller, E. W.; Williams, D. D.; Miller, R. R. High temperature vapor pressures of sodium, potassium and cesium. *J. Chem. Eng. Data* **1966**, *11*, 315–320.
(10) Stone, J. P.; Ewing, C. T.; Spann, J. R.; Steinkuller, E. W.; Williams, D. D.; Miller, R. R. High temperature *PVT* properties of sodium, potassium and cesium. *J. Chem. Eng. Data* **1966**, *11*, 309–314.
(11) Parsafar, G.; Mason, E. A. Linear isotherms for dense fluids. A new regularity. *J. Phys. Chem.* **1993**, *97*, 9048–9053.
(12) Parsafar, G.; Moeini, V.; Najafi, B. Pressure dependency liquid vapor pressure: Gibbs prediction improvement. *Iran. J. Chem. Chem. Eng.* **2001**, *20*, 37–43.
(13) Keshavarzi, E.; Parsafar, G. Prediction of the metal-nonmetal transition using the linear isotherm regularity. *J. Phys. Chem. B* **1999**, *103*, 6584–6589.
(14) Ghatee, M. H.; Bahadori, M. New thermodynamic regularity for cesium over the whole liquid range. *J. Phys. Chem. B* **2001**, *105*, 11256–11263.
(15) Ghatee, M. H.; Shams-Abadi, H. linear exp-6 isotherm for compressed molten cesium over the whole liquid range including metal-nonmetal transition and $T_C$. *J. Phys. Chem. B* **2001**, *105*, 702–710.
(16) Moore, W. J. *Basic Physical Chemistry*; Prentice/Hall international, Inc.: New York, 1983; pp 677−678.
(17) Moeini, V. A New Regularity for Internal Pressure of Dense Fluids. *J. Phys. Chem. B* **2006**, *110*, 3271–3275.
(18) Moeini, V. Internal Pressures of Lithium and Cesium Fluids at Different Temperatures. *J. Chem. Eng. Data* **2010**, *55*, 1093–1099.
(19) Hirschfelder, J. O.; Curtiss, C. F.; Bird, R. B. *Molecular Theory of Gases and Liquids*, 2nd Printing; Wiley: New York, 1964; pp 647−652.
(20) Vargaftik, N. B. *Handbook of Physical properties of Liquids and Gases*, 2nd ed.; Hemisphere: Washington, DC, 1975.
(21) Ohse, R. W. *Handbook of Thermodynamic and Transport properties of Alkali Metals*; Academic Press: Oxford, UK, 1985.
(22) Atkins, P. W. *Physical Chemistry*, 6th ed.; Oxford university press: New York, 1998; pp 84, 201−202.
(23) Matsuda, K.; Naruse, S.; Hayashi, K.; Tamura, K.; Inui, M.; Kajihara, Y. Structural study of expanded fluid cesium. *J. Phys. Conf. Ser.* **2008**, *98*, 012003.
(24) Tamura, K.; Matsuda, K.; Inui, M. structural and electronic properties of expanding fluid metals. *J. Phys.: Condens. Matter* **2008**, *20*, 114102.

Received for review June 7, 2010. Accepted November 5, 2010. We acknowledge the Payame Noor University for financial support.

JE100627C